6 *Chem. Mater.* **2005,** *17,* 6−8

Synthesis of Nanostructured Li[$Ni_{1/3}Co_{1/3}Mn_{1/3}$]O_2 via a Modified Carbonate Process

S.-H. Park,† H.-S. Shin,† S.-T. Myung,‡ C. S. Yoon,§
K. Amine,‖ and Y.-K. Sun*,†

*Department of Chemical Engineering, and Department of
Materials Science and Engineering, Center for Information
and Communication Materials, Hanyang University,
Seoul 133-791, South Korea, VK Corporation, 67 Jije-Dong,
Pyongtaek-City, Kyonggi-Do 450-090, South Korea, and
Electrochemical Technology Program, Chemical
Engineering Division, Argonne National Laboratory,
9700 South Cass Avenue, Argonne, Illinois 60439*

*Received September 10, 2004
Revised Manuscript Received November 7, 2004*

There is great deal of interest in using lithium transition-metal oxides, Li[$Ni_{1/3}Co_{1/3}Mn_{1/3}$]O_2, as the positive electrode material for high-energy and high-power lithium-ion rechargeable Li-ion secondary batteries.[1,2] Although the metallic layer of Li[$Ni_{1/3}Co_{1/3}Mn_{1/3}$]O_2 is composed of three transition metal elements, only divalent Ni and trivalent Co are electro-active through $Ni^{2+/4+}$ and $Co^{3+/4+}$ redox couples.[2,3] Tetravalent Mn, on the other hand, has a configuration of empty $3d$ e_g orbitals in octahedral coordination so that it is electrochemically inactive. However, Mn plays an essential role of supporting the host structure during Li^+ de-/intercalation.

One of the drawbacks of Li[$Ni_{1/3}Co_{1/3}Mn_{1/3}$]O_2 is that the its synthesis is not easy. An appropriate synthesis method needs to be employed, otherwise the transition metal component often saturates, resulting in oxide impurities such as NiO, Co_3O_4, Mn_2O_3, or MnO_2. Therefore, selection of an appropriate preparation method is critical to attain a final product with high purity.

Hydroxide coprecipitation proposed by Sphar et al.[4] and Davidson et al.[5] has been effective in preparing lithiated transition metal oxides with high purity. Very recently, Cho et al.[6] and Park et al.[7] also successfully prepared Li[$Ni_{1/3}Co_{1/3}Mn_{1/3}$]O_2 and Li[$Ni_{1/2}Mn_{1/2}$]O_2 based on the carbonate coprecipitation method. Electrochemical properties of the synthesized powders were satisfactory though the particle size distributions of the carbonate powder and final product were rather broad with irregular particle shapes. This lack of uniformity could be a serious drawback in the carbonate process. Here, we report electrochemical properties of nanostructured Li[$Ni_{1/3}Co_{1/3}Mn_{1/3}$]O_2 powder synthesized via a newly modified carbonate process, utilizing a chelating agent. With this new method, nanostructured Li[$Ni_{1/3}Co_{1/3}Mn_{1/3}$]O_2 powder with improved uniformity and superior rate capability can be synthesized.

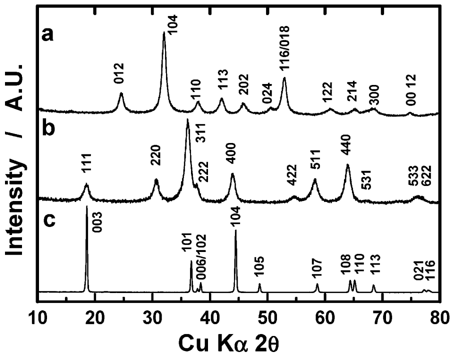

Figure 1. Powder XRD patterns of (a) as-prepared [$Ni_{1/3}Co_{1/3}Mn_{1/3}$]CO_3, (b) [$Ni_{1/3}Co_{1/3}Mn_{1/3}$]$_3O_4$ by removing CO_2 from [$Ni_{1/3}Co_{1/3}Mn_{1/3}$]CO_3, and (c) Li[$Ni_{1/3}Co_{1/3}Mn_{1/3}$]O_2 prepared by calcination of $LiNO_3$ and [$Ni_{1/3}Co_{1/3}Mn_{1/3}$]$_3O_4$.

Spherical ($Ni_{1/3}Co_{1/3}Mn_{1/3}$)CO_3 was prepared as follows. An aqueous solution of $NiSO_4$, $CoSO_4$, and $MnSO_4$ (cationic ratio of Ni/Co/Mn = 1:1:1) with a concentration of 2.0 mol dm^{-3} was pumped into a continuous stirred tank reactor (CSTR, capacity 4 L) under CO_2 atmosphere. At the same time, Na_2CO_3 solution (*aq.*) of 2.0 mol dm^{-3} and desired amount of NH_4OH solution (*aq.*) were also separately fed into the reactor. NH_3^{2+} ions are activated by a chelating agent. The solution was maintained at 60 °C for 12 h while closely monitoring the concentration of the solution (2 M), pH (7.5), temperature (60 °C), and stirring speed (1000 rpm) of the mixture. Then, the spherical ($Ni_{1/3}Co_{1/3}Mn_{1/3}$)CO_3 powder was filtered, washed, and vacuum-dried at room temperature.

Thus-prepared spherical ($Ni_{1/3}Co_{1/3}Mn_{1/3}$)CO_3 powder was dried at 110 °C to remove the adsorbed water. Then, the carbonate powder was fired at 500 °C for 5 h to decompose the carbonate into an oxide compound. Finally, a mixture containing an excess amount of $LiNO_3$ and the de-carbonated powder was preheated at 300 °C for 5 h to melt the lithium salt, and subsequently calcined at 900 °C for 20 h in air, followed by annealing at 700 °C for 5 h.

Powder X-ray diffraction (Rigaku, Rint-2000) employing Cu Kα radiation was used to identify the crystalline phase of the prepared powders at each stage. The prepared powders were also observed using scanning electron microscopy (SEM, JSM-6340F, JEOL) and transmission electron microscopy (TEM, JEM2010, JEOL). Chemical compositions of the resulting powders were analyzed with an atomic absorption spectroscopy (Vario 6, Analyticjena).

Charge−discharge tests were performed with a coin type cell (CR2032) with a current density of 20 mA g^{-1} at 30 °C. The cell consisted of a positive Li[$Ni_{1/3}Co_{1/3}Mn_{1/3}$]O_2 electrode and a negative lithium metal electrode, separated by a porous polypropylene film. The positive electrode contained 80 wt % Li[$Ni_{1/3}Co_{1/3}Mn_{1/3}$]O_2, 10% PVDF (poly-

---

* To whom correspondence should be addressed. E-mail: yksun@hanyang.ac.kr.
† Department of Chemical Engineering, Hanyang University.
‡ VK Corporation.
§ Department of Materials Science and Engineering, Hanyang University.
‖ Argonne National Laboratory.

(1) Ohzuku, T.; Makimura, Y. *Chem. Lett.* **2001**, 642.
(2) Shaju, K. M.; Subba Rao, G. V.; Chowdari, B. V. R. *Electrochim. Acta* **2002**, *48*, 145.
(3) Yoon, W.-S.; Grey, C. P.; Balasubramanian, M.; Yang, X.-Q.; McBreen, J. *Chem. Mater.* **2003**, *15*, 3161.
(4) Spahr, M. E.; Novak, P.; Schnyder, B.; Haas, O.; Nesper, R. *J. Electrochem. Soc.* **1998**, *145*, 1113.
(5) Storey, C.; Kargina, I.; Grincourt, Y.; Davidson, I. J.; Yoo, Y. C.; Seung, D. Y. *J. Power Sources* **2001**, *97*, 541.
(6) Cho, T.; Park, S.; Yoshio, M. *Chem. Lett.* **2004**, *133*, 704.
(7) Park, S.; Cho, T.; Yoshio, M. *Chem. Lett.* **2004**, *133*, *748*.

10.1021/cm048433e CCC: $30.25

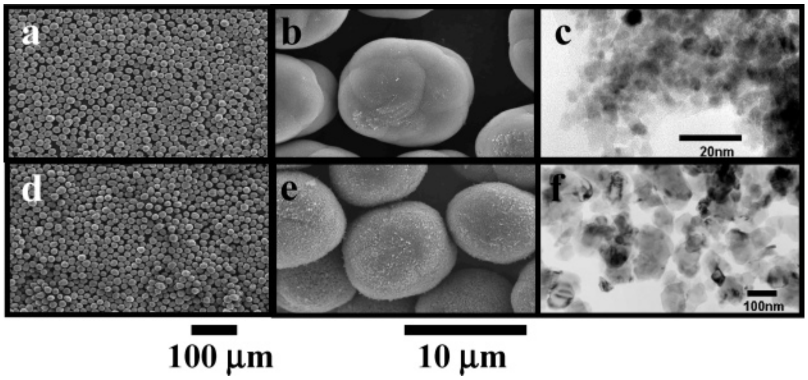

Figure 2. SEM and TEM images: (a) low- and (b) high-magnification SEM images, and (c) bright-field image of $[Ni_{1/3}Co_{1/3}Mn_{1/3}]CO_3$; (d) low- and (e) high magnification SEM images, and (f) bright-field image of $Li[Ni_{1/3}Co_{1/3}Mn_{1/3}]O_2$.

Table 1. Calculated Lattice Parameters

sample	space group	*a*-axis (Å)	*c*-axis (Å)	unit volume (Å^3)
$[Ni_{1/3}Co_{1/3}Mn_{1/3}]CO_3$	$R\bar{3}c$	4.7276(9)	15.2361(19)	294.908(15)
$[Ni_{1/3}Co_{1/3}Mn_{1/3}]_3O_4$	$Fd\bar{3}m$	8.2253(26)		556.479(11)
$Li[Ni_{1/3}Co_{1/3}Mn_{1/3}]O_2$	$R\bar{3}m$	2.8605(5)	14.2476(22)	100.962(7)

vinylidene fluoride, KURRA, Japan) binder, and 10% carbon acetylene black (Alfa Aesar Co.), which was coated on an Al foil. The electrolyte was a 1:2 mixture of ethylene carbonate (EC) and dimethyl carbonate (DMC) containing 1 M $LiPF_6$ by volume.

To prepare a homogeneous metal carbonate, it is important to control the pH of the respective metal-containing aqueous solution. In the case of Mn, especially, the pH control is very critical since precipitation of manganese oxide is favored by high temperature (>60 °C); hence, pH of the solution was increased to the range at which manganese hydroxide would not precipitate.[8]

The structure of the prepared powder was examined by XRD at each synthesis stage and the corresponding patterns are shown in Figure 1. The coprecipitated carbonate is single-phased and has a typical structure corresponding to those of $NiCO_3$, $CoCO_3$, and $MnCO_3$, all of which have divalent transition metals in their formal charge. This structure was indexed to a hexagonal structure with a space group of $R\bar{3}c$. The diffraction peaks were quite broad due to the small particle size. As can be seen in Figure 2a and b, the as-prepared carbonate particles have spherical shapes with an average diameter of 10 μm. TEM observation showed that the particles were composed of 5−8-nm sized primary particles. The spherical carbonate particles shown in Figure 2b have a unique structure in which nanosized primary particles were tightly agglomerated into a spherical shape. It was also observed that the uniformity of the secondary particle size and shapes were much improved compared to those of the previous results.[6,7] The improved uniformity was attributed to the action of the chelating agent, NH_3^{2+} ions, according to the following reaction:[9]

$$\begin{aligned} &Ni^{2+}(aq.) + Co^{2+}(aq.) + Mn^{2+}(aq.) + xNH_3^{2+} \rightarrow \\ &\quad [NiCoMn(NH_3)n^{2+}](aq.) + (x-n)NH_3^{2+}(aq) \times \\ &\quad [NiCoMn(NH_3)n^{2+}](aq.) + yCO_3^{2-} + zH_2O \rightarrow \\ &\qquad [NiCoMn]CO_3(s) + nNH_3^{2+} \end{aligned}$$

Hence, the chelating agent basically prevents the phase separation and leads to the formation of homogeneous and uniform carbonate particles as shown in Figure 2a and b. In the works by Cho et al.[6] and Park et al.[7] in which chelating agents were not used, the morphology and homogeneity of the carbonate powders were significantly inferior. The carbonate powder was fired to form $[Ni_{1/3}Co_{1/3}Mn_{1/3}]_3O_4$ (hereafter referred as precursor). After firing, the hexagonal carbonate structure changed to a cubic spinel Co_3O_4 structure as can be seen from Figure 1b. The calculated lattice constant was $a = 8.2253(26)$ Å. Calcination of the precursor with the lithium salt ($LiNO_3$) gave the phase-pure layered $Li[Ni_{1/3}Co_{1/3}Mn_{1/3}]O_2$ product as seen from Figure 1c. The calculated lattice parameters were close to those of the reported values[1−3,6] listed in Table 1. The particle size and shapes were more or less retained from the coprecipitated carbonate powder during calcination and annealing, as can be seen from Figure 2d and e. TEM confirmed that similar to the precursor, each powder particle also consisted of much finer primary particles whose sizes ranged from 50 to 100 nm as shown in Figure 2g. This is similar to what was observed in the precursor. The primary particles of $Li[Ni_{1/3}Co_{1/3}Mn_{1/3}]O_2$ were better crystallized (some of the particles were faceted) and considerably larger in size compared to the carbonate powder, which explains the increased surface roughness of the final $Li[Ni_{1/3}Co_{1/3}Mn_{1/3}]O_2$ particle in Figure 2e. It is important to note that the particles were held together by a rather weak binding force. The primary particles fell apart with low ultrasonification (Figure 2f). Such a loose structure would better accommodate any volume changes involved with structural transition or Li intercalation. There was no substantial difference in microscopic particle morphology between as-precipitated $[Ni_{1/3}Co_{1/3}Mn_{1/3}]CO_3$ and $Li[Ni_{1/3}Co_{1/3}Mn_{1/3}]O_2$ despite the structural transition, which indicates that lithium was readily incorporated into the primary structure. The initial particle morphology in the studies by Cho et al.[6] and Part et al.[7] was drastically altered by de-carbonation and high-temperature calcination. It appears that our unique nano-structured morphology of the prepared particles relieved the

---

(8) Nichols, A. R.; Walton, J. H. *J. Am. Chem. Soc.* **1942**, *64*, 1866.
(9) Lee, M.-H.; Kang, Y.-J.; Myung, S.-T.; Sun, Y.-K. *Electrochim. Acta*, in press.

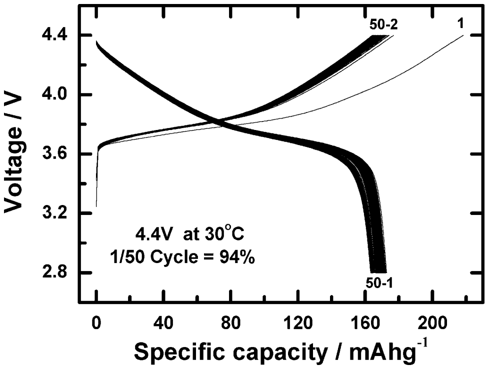

Figure 3. Continuous charge and discharge curves of Li/Li[$Ni_{1/3}Co_{1/3}Mn_{1/3}$]-O_2 cell. The applied current density was 20 mA g^{-1} at 30 °C.

stresses developed by CO_2 evolution and lithiation and helped to maintain the structural integrity. It will be shown in Figure 4 that the nanostructure also improved structural stability during Li-intercalation and deintercalation at an accelerated rate.

Figure 3 shows the cell voltage plotted versus specific gravimetric capacity for the charge and discharge of Li/Li-[$Ni_{1/3}Co_{1/3}Mn_{1/3}$]O_2 between 2.8 and 4.4 V versus Li^0 during 50 cycles. The positive electrodes are first galvanostatically charged and subsequently discharged by applying a current density of 20 mA g^{-1} at 30 °C. The Li/Li[$Ni_{1/3}Co_{1/3}Mn_{1/3}$]-O_2 cells showed monotonic voltage variations. The observed discharge capacity was 173 mAh g^{-1}. The obtained capacity was considerably higher than that obtained by Cho et al.[6] based on the cutoff voltage to 4.4 V. The sample also exhibited a smaller IR drop between charge and discharge in the whole voltage range in Figure 3. The cell exhibited very stable cyclability with high capacity of 163 mAh (g oxide)$^{-1}$ after 50 cycles as shown in Figure 3.

Rate capability tests illustrate more interesting results. As observed in Figure 4a, the Li/Li[$Ni_{1/3}Co_{1/3}Mn_{1/3}$]O_2 cell maintained its discharge capacity at high rates. At 5 C (1400 mA g^{-1}), the obtained discharge capacity is of about 85% of that of 0.2 C (56 mA g^{-1}). Figure 4b shows that the discharge capacity at high currents was well retained during cycling. This enhanced discharge capacity at accelerated rates clearly demonstrates the advantages of our nanostructured electrode. Since primary particles are held by comparatively weak secondary bonds, the volumetric changes involved with Li migration can be readily accommodated by relaxation of the binding forces among primary particles. Similar improvements in electrochemical properties by nanoscale grains and nanoscale structures have been previously reported.[10−12] However, in contrast to previous work in which the nanostructures were produced rather fortuitously by ball-milling or induced by phase transition, the nanostructured material

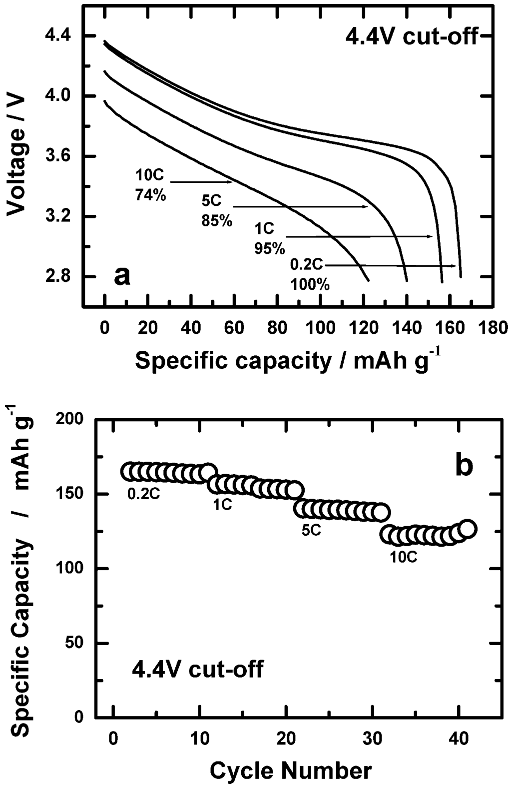

Figure 4. Rate capability of Li/Li[$Ni_{1/3}Co_{1/3}Mn_{1/3}$]O_2 cell 25 °C.

described in this work resulted from a well-controlled synthesis process, thus the morphology and its effects on electrochemical properties should be much more reproducible. In addition, its unique structure together with the uniformity should expedite the coating of the electrode onto the Al foil and reduce the necessary volume fraction of conducting agent during the battery assembly. The nano-structure morphology would also increase the contact surface between the electrolyte and electrode, enhancing the cell performance. Hence, our nanostructured morphology not only improves the structural stability of the electrode, but it is also expected to improve the overall performance of the Li battery.

The XRD result of the cycled positive electrode after 50 cycles (not shown) indicates that the cycled electrode maintained its original structure. The calculated lattice parameters after cycling were $a = 2.8604(5)$ Å, and $c = 14.2405(16)$ Å. Comparing the lattice constants from the cycled electrode to those of the pristine material in Table 1 shows that there is no large difference in the lattice parameter even after prolonged cycling, attesting to the structural stability brought about by the unique morphology and improved homogeneity of Li[$Ni_{1/3}Co_{1/3}Mn_{1/3}$]O_2 prepared via our modified carbonate process.

Acknowledgment. This work was performed by partial financial support of the "21st Century Frontier R&D programs" and "National R&D programs" of the Ministry of Science and Technology, Republic of Korea.

CM048433E

---

(10) Kang, S.-H.; Goodenough, J. B.; Rabenberg, L. K.; *Chem. Mater.* **2001**, *13*, 1758.

(11) Armstrong, A. R.; Paterson, A. J.; Robertson, A. D.; Bruce, P. G. *Chem. Mater.* **2002**, *14*, 710.

(12) Chiang, Y.-M.; Wang, H.; Jang, Y.-I. *Chem. Mater.* **2001**, *13*, 53.